IN-39
117 29
p. 38

NASA Contractor Report 4359

The Computational Structural Mechanics Testbed Structural Element Processor ES6: STAGS Beam Element

Shahram Nour-Omid, Frank Brogan,
and Gary M. Stanley

CONTRACT NAS1-18444
MAY 1991

NASA Contractor Report 4359

The Computational Structural Mechanics Testbed Structural Element Processor ES6: STAGS Beam Element

Shahram Nour-Omid, Frank Brogan,
and Gary M. Stanley
Lockheed Missiles & Space Company, Inc.
Palo Alto, California

Prepared for
Langley Research Center
under Contract NAS1-18444

NASA
National Aeronautics and
Space Administration
Office of Management
Scientific and Technical
Information Division

1991

Preface

This report documents the theory behind the CSM Testbed structural finite element processor ES6 for the STAGS beam element. The CSM Testbed is described in reference 1.

This report is intended both for CSM Testbed users, who would like theoretical background on element types before selecting them for an analysis, as well as for element researchers who are attempting to improve existing elements or to develop entirely new formulations.

Contents

List of Figures

List of Tables

1. GENERAL DESCRIPTION

1.1 Purpose

Processor ES6 contains the displacement-based 2-node beam element used within the STAGS code (ref. 2). This element is intended for modeling slender beams, which appear either in frame structures or as stiffening elements for shell structures. In STAGS, the element is referred to as the 210 element; in CSM Testbed processor ES6, it is called element E210. The E210 element in ES6 is a two-node *straight* beam element with 3 translational and 3 rotational freedoms per node. It thus represents a *faceted* approximation when used to model curved structures. The element features a cubic transverse (bending) displacement field, and linear axial and torsional displacement fields. Hence, it is considered compatible as a stiffener element with the STAGS-410 shell element, which is implemented as element E410 in CSM Testbed processor ES5. Note that the E210 beam element does not model warping deformations due to torsion, but does have a limited transverse-shear deformation capability (described in Section 2.13).

Arbitrarily large rotations (but only small strains) may be modeled with the E210 beam elements by employing the standard corotational utility available for all ES processors.

1.2 Background

Processor ES6 was developed by Frank Brogan and Shahram Nour-Omid of the Lockheed Palo Alto Research Laboratory (LPARL). The E210 element was originally developed for the STAGS code by Gary Stanley of LPARL, and recently transferred to the CSM Testbed as processor ES6, by the above authors, under the sponsorship of the NASA CSM Program.

1.3 Specific Element Types

Processor ES6 contains only one element type, the E210 beam element, which is equivalent to the 210 element within the STAGS code. For quick reference, a brief description of the ES6/E210 beam element is presented in Table 1, and an element fact sheet is provided in Table 2.

In Table 2 the following definitions apply:

NEN - number of element nodes

NIP - number of integration points

NSTR - number of stresses

NDOF - number of nodal degrees of freedom

Table 1. Summary of Processor ES6 Element Types

Type	*Description*
E210	2-node straight C^1 beam element. This is the same element available in the STAGS finite element code (where it is called the 210 element). It is recommended for general frame structures, or as a shell-stiffener element which can be used in conjunction with the E410 shell element in processor ES5.

Table 2. Element ES6/E210 Fact Sheet	
Attribute	*Description*
Element Type	2-Node C^1 Straight Beam Element
Developers	F. A. Brogan, G. M. Stanley & S. Nour-Omid (LPARL)
Topology NEN=2 NIP=2 NSTR=4 NDOF=6	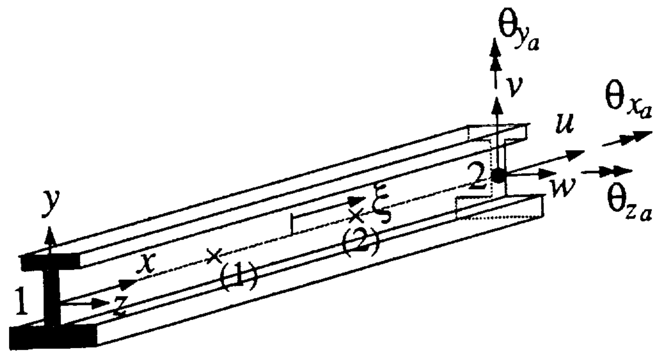 $\mathbf{d}_e^a = \left\{ \begin{matrix} \overline{\mathbf{u}}_e^a \\ \theta_e^a \end{matrix} \right\}$ $(a = 1, 2)$
Intended Use	Slender beams and shell-stiffeners
Variational Basis	Assumed displacements (Total Potential Energy)
Geometric Approx.	Straight span; normal cross-sections
Displacement Approx.	Cubic transverse $(\overline{v}, \overline{w})$; Linear axial $(\overline{u}, \alpha)$
Strain Approximation $\widetilde{\epsilon} = \{\overline{\epsilon}_x, \kappa_y, \kappa_z, \alpha\}^T$	$\overline{\epsilon}_x \sim const.$ $\kappa_y, \kappa_z \sim p_1(x)$ $\alpha \sim const.$
Stress Approximation $\widetilde{\sigma} = \{N_x, M_y, M_z, T\}^T$	Using constitutive relations, *e.g.*, $\widetilde{\sigma}(x) = \widetilde{\mathbf{C}}(x)\widetilde{\epsilon}(x)$
Force Vectors	$\mathbf{f}_e^{int} = \frac{L_e}{2} \sum_{g=1}^{2} w_g \, \mathbf{B}^T(x_g)\widetilde{\sigma}(x_g)$ $\mathbf{f}_e^{ext} = \frac{L_e}{2} \sum_{g=1}^{2} w_g \, \widetilde{\mathbf{N}}_D^T(x_g)(\widetilde{\mathbf{f}}^b(x_g) + \widetilde{\mathbf{f}}^l(x_g))$
Stiffness Matrices	$\mathbf{K}_e^{matl} = \frac{L_e}{2} \sum_{g=1}^{2} w_g \, \mathbf{B}^T(x_g)\widetilde{\mathbf{C}}(x_g)\mathbf{B}(x_g)$ $\mathbf{K}_e^{geom} = \frac{L_e}{2} \sum_{g=1}^{2} w_g \, N_x(x_g)\mathbf{G}^T(x_g)\mathbf{G}(x_g)$
Mass Matrices	$\mathbf{M}_e^C = \frac{L_e}{2} \sum_{g=1}^{2} w_g \, \widetilde{\mathbf{N}}_D^T(x_g)\mathcal{I}(x_g)\widetilde{\mathbf{N}}_D^T(x_g)$ $\mathbf{M}_e^D = diag\{(\overline{m}_1\mathbf{I}_3, \hat{m}_1\mathbf{I}_3), (\overline{m}_2\mathbf{I}_3, \hat{m}_2\mathbf{I}_3)\}$
Nonlinearity	Lagrange strains and/or corotation
Pathologies	None
Recommended Use	General-purpose applications

2. ELEMENT FORMULATION

2.1 Summary

The E210 element is a two-node beam element that features Hermitian-cubic interpolation of transverse displacements, and linear interpolation of the axial displacement and twist. The beam element is based on Bernoulli-Euler beam theory, and thus satisfies the C^1 continuity requirement, *i.e.*, first derivatives of the transverse displacements are continuous across element boundaries – for straight beam segments. Note that while transverse-shear deformations due to transverse forces are not accounted for in the basic formulation*, transverse-shear strains and stresses due to *torsion* are included – albeit without cross-sectional warping effects.

2.2 Variational Basis

The E210 element can be derived by starting with the principle of minimum total potential energy, wherein the displacements are the only independently approximated field.

2.2.1 Continuum Equations

The principle of minimum total potential energy states that:

$$\delta\Pi_T(\mathbf{u}) = 0 \tag{1}$$

where, for linear elastic analysis, Π_T is the total potential energy functional:

$$\Pi_T(\mathbf{u}) = \frac{1}{2}\int_V \epsilon(\mathbf{u})^T\,\mathbf{C}\,\epsilon(\mathbf{u})\,dV - \Big(\int_V \mathbf{u}^T\,\mathbf{f}^b\,dV + \int_S \mathbf{u}^T\,\mathbf{f}^s\,dS\Big) \tag{2}$$

in which $\mathbf{x}$ is the position vector, $\mathbf{u}(\mathbf{x})$ is the displacement vector, $\mathbf{f}^b(\mathbf{x})$ and $\mathbf{f}^s(\mathbf{x})$ are body and surface force vectors, $\mathbf{C}(\mathbf{x})$ is the constitutive matrix, and the strain operator, $\epsilon(\mathbf{u})$, is defined for linear analysis by:

$$\epsilon(\mathbf{u}) = \frac{1}{2}(\nabla\mathbf{u} + (\nabla\mathbf{u})^T) = \frac{1}{2}(\frac{\partial\mathbf{u}}{\partial\mathbf{x}} + (\frac{\partial\mathbf{u}}{\partial\mathbf{x}})^T) \tag{3}$$

which in vector notation and Cartesian components is defined as:

$$\epsilon(\mathbf{u}) = \{\epsilon_{11} \quad \epsilon_{22} \quad 2\epsilon_{12} \quad 2\epsilon_{31} \quad 2\epsilon_{32} \quad \epsilon_{33}\}^T \tag{4}$$

We have assumed (for the time being) that the stress tensor is related to the strain tensor by

$$\boldsymbol{\sigma} = \mathbf{C}\,\boldsymbol{\epsilon} \tag{5}$$

---

* See Section 2.13 for a description of a limited transverse-shear deformation capability.

where in vector notation and Cartesian components:

$$\sigma = \{\sigma_{11} \quad \sigma_{22} \quad \sigma_{12} \quad \sigma_{31} \quad \sigma_{32} \quad \sigma_{33}\}^T \tag{6}$$

2.2.2 Beam Assumptions

The geometry of a generally curved beam in space is illustrated in Figure 1; the E210 element formulation is based upon the projection of the general curve onto a straight segment (see figure). The following assumptions are introduced into the continuum variational equations to obtain corresponding "beam" variational equations – and hence reduce the above volume integrals to line integrals:

1) Plane sections remain plane *and* normal to the beam neutral axis.
2) Beam transverse-normal stresses $(\sigma_{yy}, \sigma_{zz})$ and lateral-shear stresses (σ_{yz}) can be neglected.

Thus, the displacement field for a generic point in the beam may be decomposed into translational and rotational components as follows:

$$\boxed{\begin{aligned} u(x,y,z) &= \bar{u}(x) - y\theta_z(x) + z\theta_y(x) \\ v(x,y,z) &= \bar{v}(x) - z\theta_x(x) \\ w(x,y,z) &= \bar{w}(x) + y\theta_x(x) \end{aligned}} \tag{7}$$

where x is the axial coordinate, y and z are the cross-section coordinates, $\overline{u}$, $\overline{v}$, $\overline{w}$ are the displacements (translations) in the x, y, z directions at the beam reference axis, and θ_x, θ_y, θ_z are the rotations of the cross-section about the x, y, z axes, respectively. (The sign convention for rotations follows the right-hand rule.)

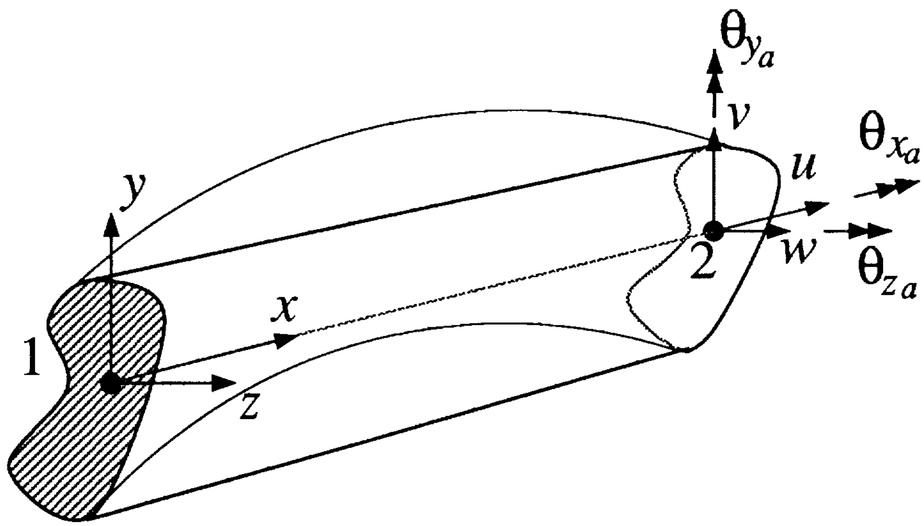

Figure 1. Beam Geometry Used in ES6/E210 Element Formulation

Note that the "plane-sections remain *normal*" assumption engenders the following dependency relationship between the rotation components θ_y, θ_z and derivatives of the transverse displacements $\overline{v}, \overline{w}$:

$$\boxed{\begin{aligned} \theta_y &= -\overline{w}_{,x} \\ \theta_z &= \overline{v}_{,x} \end{aligned}} \tag{8}$$

where the commas denote differentiation. It is convenient to re-express equation (7) using the following matrix/vector notation:

$$\boxed{\mathbf{u}(x,y,z) \;=\; \overline{\mathbf{u}}(x) \;+\; \mathbf{A}(y,z)\,\boldsymbol{\theta}(x)} \tag{9}$$

where

$$\mathbf{u} = \left\{ \begin{array}{c} u \\ v \\ w \end{array} \right\}, \qquad \overline{\mathbf{u}} = \left\{ \begin{array}{c} \overline{u} \\ \overline{v} \\ \overline{w} \end{array} \right\}, \qquad \boldsymbol{\theta} = \left\{ \begin{array}{c} \theta_x \\ \theta_y \\ \theta_z \end{array} \right\} \tag{10}$$

and

$$\mathbf{A} \;=\; \begin{array}{c} \\ u \\ v \\ v \end{array} \!\!\begin{array}{c} \begin{array}{ccc} \theta_x & \theta_y & \theta_z \end{array} \\ \begin{pmatrix} 0 & z & -y \\ -z & 0 & 0 \\ y & 0 & 0 \end{pmatrix} \end{array} \tag{11}$$

Substituting equation (9) into equation (2) yields the beam total potential energy functional:

$$\boxed{\widetilde{\Pi}_T(\widetilde{\mathbf{u}}) \;=\; \frac{1}{2}\int_0^L \widetilde{\boldsymbol{\epsilon}}(\widetilde{\mathbf{u}})^T\,\widetilde{\mathbf{C}}\,\widetilde{\boldsymbol{\epsilon}}(\widetilde{\mathbf{u}}) \;-\; \int_0^L \widetilde{\mathbf{u}}^T\,(\widetilde{\mathbf{f}}^b + \widetilde{\mathbf{f}}^\ell)} \tag{12}$$

where the superposed tildes represent beam resultant quantities, defined as follows:

$$\widetilde{\mathbf{u}}(x) \;=\; \{\overline{\mathbf{u}}(x),\; \boldsymbol{\theta}(x)\}^T \;=\; \textit{Resultant Displacement Vector} \tag{13}$$

$$\widehat{\boldsymbol{\epsilon}}(x,y,z) \;=\; \mathbf{A}_{\boldsymbol{\epsilon}}(\mathbf{y},\mathbf{z})\,\widetilde{\boldsymbol{\epsilon}}(\mathbf{x}) \;=\; \textit{Reduced Strain Vector} \tag{14}$$

$$\widetilde{\boldsymbol{\sigma}}(x) \;=\; \int_A \mathbf{A}_{\boldsymbol{\epsilon}}^{\mathbf{T}}(\mathbf{y},\mathbf{z})\,\widehat{\boldsymbol{\sigma}}(\mathbf{x},\mathbf{y},\mathbf{z}) \;=\; \textit{Resultant Stress Vector} \tag{15}$$

$$\widetilde{\mathbf{C}}(x) \;=\; \int_A \mathbf{A}_{\boldsymbol{\epsilon}}^{\mathbf{T}}(\mathbf{y},\mathbf{z})\,\widehat{\mathbf{C}}(\mathbf{x},\mathbf{y},\mathbf{z})\,\mathbf{A}_{\boldsymbol{\epsilon}}(\mathbf{y},\mathbf{z}) \;=\; \textit{Resultant Constitutive Matrix} \tag{16}$$

$$\mathbf{A}_{\boldsymbol{\epsilon}}(\mathbf{y},\mathbf{z}) \;=\; \begin{bmatrix} 1 & y & z & 0 \\ 0 & 0 & 0 & -z \\ 0 & 0 & 0 & y \end{bmatrix} \;=\; \textit{Strain Partitioning Matrix} \tag{17}$$

$$\tilde{\mathbf{f}}^b(x) = \int_A \left\{ \begin{array}{c} \mathbf{f}^b(x,y,z) \\ \mathbf{A}^T(y,z)\,\mathbf{f}^b(x,y,z) \end{array} \right\} = \left\{ \begin{array}{c} \bar{\mathbf{f}}^b(x) \\ \mathbf{m}^b(x) = 0 \end{array} \right\} = \textit{Resultant Body-Load Vector} \tag{18}$$

$$\tilde{\mathbf{f}}^\ell(x) = \left\{ \begin{array}{c} \mathbf{f}^\ell(x,y_\ell,z_\ell) \\ \mathbf{A}^T(y_\ell,z_\ell)\,\mathbf{f}^\ell(x,y_\ell,z_\ell) \end{array} \right\} = \left\{ \begin{array}{c} \bar{\mathbf{f}}^\ell(x) \\ \mathbf{m}^\ell(x) \end{array} \right\} = \textit{Resultant Line-Load Vector} \tag{19}$$

where y_ℓ, z_ℓ are the cross-section coordinates defining the surface of the beam upon which line loads, $\mathbf{f}^\ell$, are applied.

The "hats" above the quantities, $\widehat{\boldsymbol{\epsilon}}, \widehat{\boldsymbol{\sigma}}$ and $\widehat{\mathbf{C}}$, in equations (14)-(16) denote enforcement of beam assumption 1), namely:

$$\sigma_{yy} = \sigma_{zz} = \sigma_{yz} = 0 \tag{20}$$

which enables reduction of the 3-D continuum stress and strain arrays appearing in equations (4)-(6) from 6 to 3, *i.e.*,

$$\widehat{\boldsymbol{\epsilon}}(x,y,z) = \left\{ \begin{array}{c} \epsilon_{xx}(x,y,z) \\ 2\epsilon_{xy}(x,y,z) \\ 2\epsilon_{xz}(x,y,z) \end{array} \right\} \quad \text{and} \quad \widehat{\boldsymbol{\sigma}}(x,y,z) = \left\{ \begin{array}{c} \sigma_{xx}(x,y,z) \\ \sigma_{xy}(x,y,z) \\ \sigma_{xz}(x,y,z) \end{array} \right\} \tag{21}$$

such that the reduced linear-elastic constitutive matrix becomes:

$$\widehat{\mathbf{C}}(x,y,z) = \begin{array}{c c} & \begin{array}{ccc} \epsilon_{xx} & 2\epsilon_{xy} & 2\epsilon_{xz} \end{array} \\ \begin{array}{c} \sigma_{xx} \\ \sigma_{xy} \\ \sigma_{xz} \end{array} & \begin{pmatrix} E & 0 & 0 \\ 0 & G & 0 \\ 0 & 0 & G \end{pmatrix} \end{array} \tag{22}$$

where E and G are the elastic and shear modulii, respectively.

Beam Resultant Strain Measures ($\widetilde{\epsilon}$)

The beam resultant strain measures emanate from equation (14), which in turn is obtained by substituting the beam kinematic hypotheses (eq. (9)) into the continuum strain-displacement relations (eq. 7)). This yields:

$$\underbrace{\left\{\begin{array}{c} \epsilon_{xx}(x,y,z) \\ 2\epsilon_{xy}(x,y,z) \\ 2\epsilon_{xz}(x,y,z) \end{array}\right\}}_{\widehat{\epsilon}(x,y,z)} = \underbrace{\begin{bmatrix} 1 & z & y & 0 \\ 0 & 0 & 0 & -z \\ 0 & 0 & 0 & y \end{bmatrix}}_{\mathbf{A}_{\epsilon}(y,z)} \underbrace{\left\{\begin{array}{c} \bar{\epsilon}_x(x) \\ \kappa_y(x) \\ \kappa_z(x) \\ \alpha(x) \end{array}\right\}}_{\widetilde{\epsilon}(x)} \quad (23)$$

where the resultant strain measures are defined as follows:

$$\boxed{\widetilde{\epsilon} = \left\{\begin{array}{c} \bar{\epsilon}_x \\ \kappa_y \\ \kappa_z \\ \alpha \end{array}\right\} = \left\{\begin{array}{c} \text{axial strain} \\ \text{bending strain due to } \theta_y \\ \text{bending strain due to } \theta_z \\ \text{twisting strain} \end{array}\right\} = \left\{\begin{array}{c} \overline{u}_{,x} \\ -\overline{w}_{,xx} \\ -\overline{v}_{,xx} \\ \theta_{,x} \end{array}\right\} = \left\{\begin{array}{c} \overline{u}_{,x} \\ \theta_{y,x} \\ -\theta_{z,x} \\ \theta_{x,x} \end{array}\right\}} \quad (24)$$

Beam Stress Resultants ($\widetilde{\sigma}$)

The beam stress resultants emanate from equation (15), which yields:

$$\boxed{\widetilde{\sigma} = \left\{\begin{array}{c} N_x \\ M_y \\ M_z \\ T \end{array}\right\} = \left\{\begin{array}{c} \text{axial force} \\ \text{bending moment about } y \\ \text{bending moment about } z \\ \text{torsional moment (about } x) \end{array}\right\} = \int_A \left\{\begin{array}{c} \sigma_{xx} \\ \sigma_{xx}\, z \\ \sigma_{xx}\, y \\ (\sigma_{xz}\, y - \sigma_{xy}\, z) \end{array}\right\}} \quad (25)$$

Beam Resultant Constitutive Matrix ($\widetilde{\mathbf{C}}$)

The beam resultant linear-elastic constitutive matrix relating $\widetilde{\sigma}(x)$ and $\widetilde{\epsilon}(x)$ emanates from equation (16), which expands to:

$$\boxed{\widetilde{\mathbf{C}} = \begin{array}{c} \\ N_x \\ M_y \\ M_z \\ T \end{array} \begin{array}{c} \begin{array}{cccc} \bar{\epsilon}_x & \kappa_y & \kappa_z & \alpha \end{array} \\ \begin{pmatrix} \int_A E & \int_A Ez & \int_A Ey & 0 \\ \int_A Ez & \int_A Ez^2 & \int_A Eyz & 0 \\ \int_A Ey & \int_A Eyz & \int_A Ey^2 & 0 \\ 0 & 0 & 0 & \int_A G(y^2+z^2) \end{pmatrix} \end{array}} \quad (26)$$

In particular, if the beam cross-section is homogeneous, then $\widetilde{\mathbf{C}}$ becomes:

$$\widetilde{\mathbf{C}} = \begin{array}{c} \\ N_x \\ M_y \\ M_z \\ T \end{array} \begin{array}{c} \begin{array}{cccc} \quad\bar{\epsilon}_x & \quad\kappa_y & \quad\kappa_z & \quad\alpha \end{array} \\ \begin{pmatrix} EA & EAe_z & EAe_y & 0 \\ EAe_z & EI_{zz} & EI_{yz} & 0 \\ EAe_y & EI_{yz} & EI_{yy} & 0 \\ 0 & 0 & 0 & GJ \end{pmatrix} \end{array} \tag{27}$$

where the cross-section geometric properties are defined by:

$$A = \int_A = Area \tag{28}$$

$$e_y = \frac{\int_A y}{A} = Eccentricity\ in\ y\ Direction \tag{29}$$

$$e_z = \frac{\int_A z}{A} = Eccentricity\ in\ z\ Direction \tag{30}$$

$$I_{yy} = \int_A y^2 = Moment\text{-}of\text{-}Inertia\ about\ z\ Axis \tag{31}$$

$$I_{zz} = \int_A z^2 = Moment\text{-}of\text{-}Inertia\ about\ y\ Axis \tag{32}$$

$$I_{yz} = \int_A yz = Product\text{-}of\text{-}Inertia \tag{33}$$

$$J = \int_A (y^2 + z^2) = Polar\ Moment\text{-}of\text{-}Inertia \tag{34}$$

2.3 Discrete Equations

The finite element beam equations are obtained from equation (12) by introducing intra-element approximations for the geometry and displacement field of the form:

$$\mathbf{x}(x) = \mathbf{N}_G(x)\,\mathbf{x}^e \tag{35a}$$

$$\tilde{\mathbf{u}}(x) = \tilde{\mathbf{N}}_D(x)\,\mathbf{d}^e \tag{35b}$$

where

$$\mathbf{x}^e = \begin{Bmatrix} \mathbf{x}_1^e \\ \mathbf{x}_2^e \end{Bmatrix} \qquad \text{and} \qquad \mathbf{d}^e = \begin{Bmatrix} \mathbf{d}_1 \\ \mathbf{d}_2 \end{Bmatrix}$$

are the expanded element nodal coordinate and nodal displacement vectors, respectively, and x is now the beam-element axial coordinate which ranges from $(0, L_e)$, where L_e is the element length. With the above discrete approximations, to be defined in detail in subsequent sections, the strain resultant vector becomes:

$$\begin{aligned} \tilde{\boldsymbol{\epsilon}}(x) &= \tilde{\boldsymbol{\epsilon}}\left(\tilde{\mathbf{N}}_D(x)\,\mathbf{d}^e\right) \\ &= \mathbf{B}(x)\,\mathbf{d}^e \end{aligned} \tag{36}$$

where $\mathbf{B}$ is the element strain-displacement matrix, defined by substituting the above element displacement approximations (eq. (35b)) into the beam strain-displacement relations (eq. (24)).

The discrete form of the variational functional (eq. (12)) becomes:

$$\Pi_T = \sum_{e=1}^{Nel} \Pi_T^e \tag{37}$$

where the script e denotes an individual element, Nel is the total number of elements, and the element total potential energy may be expressed as:

$$\Pi_T^e = \frac{1}{2}\mathbf{d}_e^T\,\mathbf{K}_e^{matl}\,\mathbf{d}_e - \mathbf{d}_e^T\,\mathbf{f}_e^{ext} \tag{38}$$

In equation (38) $\mathbf{K}_e^{matl}$ is the element *material* (or linear) stiffness matrix, and $\mathbf{f}_e^{ext}$ is the element external force vector, defined as follows:

$$\mathbf{K}_e^{matl} = \mathbf{T}_{EC}^T \left(\int_0^{Le} \overline{\mathbf{B}}^T\,\tilde{\mathbf{C}}\,\overline{\mathbf{B}} \right) \mathbf{T}_{EC} \tag{39}$$

$$\mathbf{f}_e^{ext} = \mathbf{T}_{EC}^T \left(\int_0^{Le} \tilde{\mathbf{N}}_D^T (\tilde{\mathbf{f}}^b + \tilde{\mathbf{f}}^\ell) \right) \tag{40}$$

where $\mathbf{T}_{EC}$ is the block-diagonal transformation matrix relating the computational basis at each element node to the element local Cartesian basis. Specific equation systems emanating from equations (37)-(38), and their generalizations, are described in the following sections.

2.3.1 Linear Static Equations

The discrete equations for linear statics are obtained by taking the first variation of equation (37) and setting it equal to zero, *i.e.*,

$$\mathbf{K}^{matl}\,\mathbf{d} \;=\; \mathbf{f}^{ext} \tag{41}$$

where $\mathbf{K}^{matl}$ and $\mathbf{f}^{ext}$ are the assembled versions of the element material stiffness and external force vector (eqs. (39) and (40)), and $\mathbf{d}$ is the system displacement vector, composed of the union of all nodal displacement vectors.

2.3.2 Linear Dynamic Equations

For linear dynamics, an inertial term is added to the left-hand side of equation (41) – using Hamilton's principle – resulting in:

$$\mathbf{M}\,\ddot{\mathbf{d}} \;+\; \mathbf{K}^{matl}\,\mathbf{d} \;=\; \mathbf{f}^{ext} \tag{42}$$

where $\mathbf{M}$ is the structure mass matrix, assembled from the element mass matrices, $\mathbf{M}_e$, which are defined in Section 2.11.

2.3.3 Linear Eigenproblems

For linear vibration analysis, the right-hand-side of equation (42) becomes zero and we have the eigenproblem:

$$\left(\mathbf{K}^{matl} \;+\; \lambda\,\mathbf{M}\right)\mathbf{d}_\lambda \;=\; \mathbf{0} \tag{43}$$

where the eigenvalue, λ, is the natural frequency squared, and $\mathbf{d}_\lambda$ is the corresponding vibration mode vector.

For linear stability, or buckling analysis, $\mathbf{M}$ in equation (43) is replaced with the geometric stiffness matrix, *i.e.*,

$$\left(\mathbf{K}^{matl} \;+\; \lambda\,\mathbf{K}^{geom}(\sigma_0\right)\mathbf{d}_\lambda \;=\; \mathbf{0} \tag{44}$$

where the eigenvalue, λ, is the load multiplier associated with the pre-buckling stress, σ_0; $\mathbf{d}_\lambda$ is the corresponding buckling mode; and $\mathbf{K}^{geom}$ is the geometric stiffness matrix, defined at the element level ($\mathbf{K}_e^{geom}$) in Section 2.10.

2.3.4 Nonlinear Problems

See Section 2.12 for a description of ES6 element contributions to nonlinear equation systems.

2.4 Element Topology

The topology of the E210 beam element is shown in Figure 2.

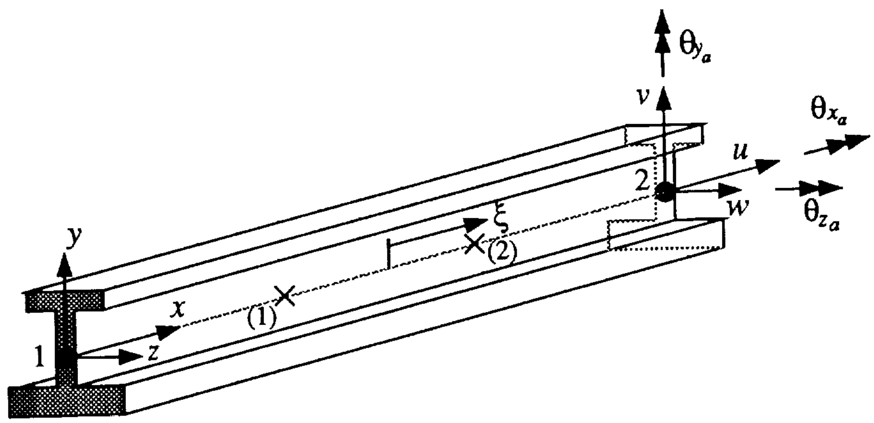

Figure 2. Topology of the E210 Beam Element

Each node possesses the 6 displacement degrees of freedom:

$$\mathbf{d}_a = \left\{ \begin{array}{c} \overline{\mathbf{u}}_a \\ \boldsymbol{\theta}_a \end{array} \right\} \tag{45}$$

where:

$$\overline{\mathbf{u}}_a = \left\{ \begin{array}{c} \overline{u}_a \\ \overline{v}_a \\ \overline{w}_a \end{array} \right\} \quad \text{and} \quad \boldsymbol{\theta}_a = \left\{ \begin{array}{c} \theta_{xa} \\ \theta_{ya} \\ \theta_{za} \end{array} \right\} \tag{46}$$

are the translation and rotation components at element node a, expressed in the fixed element local x, y, z coordinate system (in which x is the projected straight-beam span direction).

Each element also stores the 4 resultant stress and/or strain components defined in equations (24) and (25) at each of the two Gauss integration points illustrated in Figure 2, and tabulated in Table 3.

Table 3. Gauss Integration Coordinates/Weights for E210 Beam Element			
Integ. Pt. (g)	*Natural Coord.*(ξ_g)	*Physical Coord.*(x_g)	*Weight*(w_g)
1	$-1/\sqrt{3}$	$\left(\frac{1-1/\sqrt{3}}{2}\right)L_e$	1
2	$+1/\sqrt{3}$	$\left(\frac{1+1/\sqrt{3}}{2}\right)L_e$	1

2.5 Geometric Approximations

The element geometry, illustrated in Figure 2 and embodied in equation (35a), is approximated within the element by linearly interpolating the position vectors on the beam reference axis from nodal values, *i.e.*,

$$\mathbf{x}(x) \;=\; \sum_{a=1}^{2} N_a^L(x)\,\mathbf{x}_a \tag{47}$$

where

$$N_1^L(x) \;=\; 1 - \frac{x}{L_e} \qquad \text{and} \qquad N_2^L(x) \;=\; \frac{x}{L_e} \tag{48}$$

are the linear Lagrange interpolation functions, expressed in terms of the physical coordinate x. Thus, the element reference axis is represented by a straight line, and a span-wise assemblage of E210 beam elements results in a piecewise straight approximation of a generally curved beam.

The above expression may be recast in the matrix notation of equation (35a) as follows:

$$\mathbf{x}(x) \;=\; \mathbf{N}_G(x)\,\mathbf{x}^e \tag{49}$$

where

$$\mathbf{N}_G(x) \;=\; [\,N_1^L(x)\mathbf{I}_3 \quad N_2^L(x)\mathbf{I}_3\,]$$

Note that the physical span coordinate, x, can be expressed in terms of the *natural* coordinate ξ – for purposes of numerical integration – by the relationship:

$$x(\xi) \;=\; \frac{(1+\xi)}{2}\,L_e \tag{50}$$

where ξ ranges from -1 to +1, as x ranges from 0 to L_e.

2.6 Displacement Approximations

The ES6/E210 beam element uses linear Lagrange interpolation for axial displacements and torsional rotations, and cubic Hermite interpolation for transverse (bending) displacements.

2.6.1 Axial and Torsional Displacement Field

In both the axial and torsional displacement fields, $\overline{u}(x)$ and $\theta_x(x)$, respectively, the interior translations and rotations are linearly interpreted from corresponding nodal values, as follows:

$$\overline{u}(x) = \sum_{a=1}^{2} N_a^L(x)\,\overline{u}_a \tag{51}$$

$$\theta_x(x) = \sum_{a=1}^{2} N_a^L(x)\,\theta_{xa} \tag{52}$$

where the linear Lagrange shape functions and their derivatives (which will be used to compute axial and torsional strains) are given in Table 4.

Table 4. E210 Beam-Element Axial Interpolation Fns.	
(Linear Lagrange Polynomials)	
Node 1	**Node 2**
$N_1^L(x) = 1 - \frac{x}{L_e}$	$N_2^L(x) = \frac{x}{L_e}$
$N_{1,x}^L(x) = -\frac{1}{L_e}$	$N_{2,x}^L(x) = \frac{1}{L_e}$

2.6.2 Bending Displacement Field

The bending displacement field is approximated by interpolating the transverse translations, $\overline{v}(x)$ and $\overline{w}(x)$, from corresponding nodal translations *and* rotations, using cubic Hermite interpolation functions. Specifically:

$$\overline{v}(x) = \sum_{a=1}^{2} \left(\overline{N}_a^H(x)\, \overline{v}_a + \widehat{N}_a^H(x)\, \theta_{za} \right) \tag{53}$$

$$\overline{w}(x) = \sum_{a=1}^{2} \left(\overline{N}_a^H(x)\, \overline{w}_a - \widehat{N}_a^H(x)\, \theta_{ya} \right) \tag{54}$$

where $\overline{N}_a^H(x)$ is the Hermite interpolation function associated with the translations at node a, and $\widehat{N}_a^H(x)$ is the Hermite interpolation function associated with the rotations at node a. Note that the negative sign in equation (54) is due to the fact that the Hermite polynomials, $\widehat{N}_a^H(x)$, are really associated with the slopes, $\overline{v}_{,xa}$ or $\overline{w}_{,xa}$, which are related to the engineering rotations by:

$$\begin{Bmatrix} \theta_{ya} \\ \theta_{za} \end{Bmatrix} = \begin{bmatrix} 0 & -1 \\ 1 & 0 \end{bmatrix} \begin{Bmatrix} \overline{v}_{,xa} \\ \overline{w}_{,xa} \end{Bmatrix} \tag{55}$$

Similarly, the interior rotations, $\theta_y(x)$ and $\theta_z(x)$, are related to the interior slopes using:

$$\begin{Bmatrix} \theta_{y} \\ \theta_{z} \end{Bmatrix} = \begin{bmatrix} 0 & -1 \\ 1 & 0 \end{bmatrix} \begin{Bmatrix} \overline{v}_{,x} \\ \overline{w}_{,x} \end{Bmatrix} \tag{56}$$

Thus, the interior rotations may be obtained simply by differentiating equations (53)-(54) with respect to x. Note that while the *interior* rotations are *dependent* on the interior translations using equation (56), the *nodal* rotations and translations are considered *independent* variables.

The Hermite interpolation functions and their first and second derivatives (which will be used to compute bending strains) are given in Table 5.

Table 5. E210 Beam-Element Bending Interpolation Functions	
(Cubic Hermite Polynomials)	
Node 1	**Node 2**
$\overline{N}_1^H(x) = 1 - 3(\frac{x}{L_e})^2 + 2(\frac{x}{L_e})^3$ $\widehat{N}_1^H(x) = x(1 - \frac{x}{L_e})^2$	$\overline{N}_2^H(x) = 3(\frac{x}{L_e})^2 - 2(\frac{x}{L_e})^3$ $\widehat{N}_2^H(x) = \frac{x^2}{L_e}(\frac{x}{L_e} - 1)$
$\overline{N}_{1,x}^H(x) = -\frac{6x}{L_e^2}(1 - \frac{x}{L_e})$ $\widehat{N}_{1,x}^H(x) = (1 - \frac{x}{L_e})^2 - 2\frac{x}{L_e}(1 - \frac{x}{L_e})$	$\overline{N}_{2,x}^H(x) = 6\frac{x}{L_e^2}(1 - \frac{x}{L_e})$ $\widehat{N}_{2,x}^H(x) = 3(\frac{x}{L_e})^2 - 2(\frac{x}{L_e})$
$\overline{N}_{1,xx}^H(x) = -\frac{6}{L_e^2}(1 - 2\frac{x}{L_e})$ $\widehat{N}_{1,xx}^H(x) = -\frac{2}{L_e}(2 - \frac{x}{L_e})$	$\overline{N}_{2,xx}^H(x) = \frac{6}{L_e^2}(1 - 2\frac{x}{L_e})$ $\widehat{N}_{2,xx}^H(x) = \frac{2}{L_e}(3\frac{x}{L_e} - 1)$

2.6.3 Combined Displacement Field

The complete displacement field for the E210 beam element may be assembled from the above axial, torsional and bending contributions (eqs. (51)-(54)) as follows:

$$\boxed{\underbrace{\begin{Bmatrix} \overline{u}(x) \\ \overline{v}(x) \\ \overline{w}(x) \\ \theta_x(x) \\ \theta_y(x) \\ \theta_z(x) \end{Bmatrix}}_{\widetilde{\mathbf{u}}(x)} = \sum_{a=1}^{2} \underbrace{\begin{array}{c} \begin{array}{cccccc} \overline{u}_a & \overline{v}_a & \overline{w}_a & \theta_{xa} & \theta_{ya} & \theta_{za} \end{array} \\ \begin{pmatrix} N_a^L(x) & 0 & 0 & 0 & 0 & 0 \\ 0 & \overline{N}_a^H(x) & 0 & 0 & 0 & \widehat{N}_a^H(x) \\ 0 & 0 & \overline{N}_a^H(x) & 0 & -\widehat{N}_a^H(x) & 0 \\ 0 & 0 & 0 & N_a^L(x) & 0 & 0 \\ 0 & 0 & -\overline{N}_{a,x}^H(x) & 0 & \widehat{N}_{a,x}^H(x) & 0 \\ 0 & \overline{N}_{a,x}^H(x) & 0 & 0 & 0 & \widehat{N}_{a,x}^H(x) \end{pmatrix} \end{array}}_{\widetilde{\mathbf{N}}_a^D(x)} \underbrace{\begin{Bmatrix} \overline{u}_a \\ \overline{v}_a \\ \overline{w}_a \\ \theta_{xa} \\ \theta_{ya} \\ \theta_{za} \end{Bmatrix}}_{\mathbf{d}_a}} \tag{57}$$

where the Lagrange and Hermite interpolation functions (N_a^L and N_a^H) are defined in Tables 4 and 5, respectively. The above matrix, $\widetilde{\mathbf{N}}_a^D$, is used to construct the element external force vector and consistent mass matrix. Its derivatives are used to approximate the element strain field, as shown in the next section.

Finally note that equation (57) may be rewritten as:

$$\widetilde{\mathbf{u}}(x) = \widetilde{\mathbf{N}}^D(x)\,\mathbf{d}^e \tag{58}$$

where $\widetilde{\mathbf{N}}_a^D$ represents a nodal block of $\widetilde{\mathbf{N}}^D$, *i.e.*,

$$\widetilde{\mathbf{N}}^D(x) = \left[\widetilde{\mathbf{N}}_1^D(x) \quad \widetilde{\mathbf{N}}_2^D(x)\right] \tag{59}$$

2.7 Strain Approximations

The ES6/E210 beam-element strains are obtained within the interior of the element, at the standard two Gauss integration points, by substituting the above displacement approximation (eq. (57)) into the beam strain-displacement relations (eq. (24)). This yields the conventional element strain-displacement matrix, $\mathbf{B}(x)$, which is defined as follows:

$$\begin{aligned} \tilde{\epsilon}(x) &= \mathbf{B}(x)\,\mathbf{d}^e \\ &= [\mathbf{B}_1(x) \quad \mathbf{B}_2(x)] \begin{Bmatrix} \mathbf{d}_1^e \\ \mathbf{d}_2^e \end{Bmatrix} = \sum_{a=1}^{2} \mathbf{B}_a(x)\,\mathbf{d}_a^e \end{aligned} \tag{60}$$

where each of the two nodal blocks is defined as:

$$\mathbf{B}_a(x) = \begin{array}{c} \\ \bar{\epsilon}_x \\ \kappa_y \\ \kappa_z \\ \alpha \end{array} \begin{array}{c} \begin{array}{cccccc} \bar{u}_a & \bar{v}_a & \bar{w}_a & \theta_{xa} & \theta_{ya} & \theta_{za} \end{array} \\ \begin{pmatrix} N^L_{a,x} & 0 & 0 & 0 & 0 & 0 \\ 0 & 0 & -\overline{N}^H_{a,xx} & 0 & \widehat{N}^H_{a,xx} & 0 \\ 0 & -\overline{N}^H_{a,xx} & 0 & 0 & 0 & -\widehat{N}^H_{a,xx} \\ 0 & 0 & 0 & N^L_{a,x} & 0 & 0 \end{pmatrix} \end{array} \tag{61}$$

The derivatives of the Lagrange and Hermite polynomials, $N_a^L(x)$ and $N_a^H(x)$, appearing in equation (61) are given in Tables 4 and 5, respectively. Table 6 indicates how each strain component varies along the beam element length.

Table 6. Strain Variation within ES6 Elements

Strain		*Element Type*
Component		**E210 Beam Element**
Axial	$\bar{\epsilon}_x$	$p_0(x)$ – constant
Bending	κ_y	$p_1(x)$ – linear
	κ_z	$p_1(x)$ – linear
Torsional	α_x	$p_0(x)$ – constant

The element strain-displacement matrix, $\mathbf{B}$, appears in the definition of the element internal-force vector and material-stiffness matrix, given in Sections 2.9 and 2.10, respectively.

2.8 Stress Approximations

Since the E210 element within processor ES6 assumes the form of the displacement field, and strains are computed by satisfaction of the strain-displacement relations, stresses are therefore computed directly in terms of strains using the constitutive relations. For linear-elastic analysis, this amounts to:

$$\tilde{\sigma}(x) = \tilde{\mathbf{C}}(x)\tilde{\epsilon}(x) \tag{62}$$

where the location x typically corresponds to an element integration point (x_g).

2.9 Force Vectors

All element force vectors are constructed using 2-point Gauss integration. This integration rule is exact for geometrically linear analysis (with up to linearly varying section properties), but only approximate for geometrically nonlinear analysis. The reason for using this "reduced" integration rule (instead of, for example, the 3-point rule) for nonlinear analysis is that it improves solution accuracy without engendering any spurious modes.

2.9.1 Internal Force Vector

The element internal force vector is defined as:

$$\begin{aligned} \mathbf{f}_e^{int} &= \int_0^L \mathbf{B}^T \tilde{\sigma} \\ &\approx \frac{L_e}{2} \sum_{g=1}^{2} w_g \left(\mathbf{B}^T(x_g)\tilde{\sigma}(x_g) \right) \end{aligned} \tag{63}$$

where w_g and x_g are defined in Table 3, $\mathbf{B}$ is defined in equation (61), and $\tilde{\sigma}$ is defined in equation (62). Note that for linear analysis, the above definition is equivalent to $\mathbf{f}^{int} = \mathbf{K}_e^{matl}\mathbf{d}_e$.

2.9.2 External Force Vector

$$\mathbf{f}_e^{ext} = \mathbf{f}_e^{body} + \mathbf{f}_e^{line} \tag{64}$$

where the element *body force* vector is defined as:

$$\begin{aligned} \mathbf{f}_e^{body} &= \int_0^L \tilde{\mathbf{N}}_D^T \tilde{\mathbf{f}}^b \\ &\approx \frac{L_e}{2} \sum_{g=1}^{2} w_g \left(\tilde{\mathbf{N}}_D^T(x_g)\tilde{\mathbf{f}}^b(x_g) \right) \end{aligned} \tag{65}$$

and the element *line force* vector is defined as:

$$\begin{aligned} \mathbf{f}_e^{line} &= \int_0^L \widetilde{\mathbf{N}}_D^T \widetilde{\mathbf{f}}^{\ell} \\ &\approx \frac{L_e}{2} \sum_{g=1}^{2} w_g \left(\widetilde{\mathbf{N}}_D^T(x_g) \widetilde{\mathbf{f}}^{\ell}(x_g) \right) \end{aligned} \tag{66}$$

in which $\widetilde{\mathbf{N}}$ is defined in equation (57), $\mathbf{f}^b$ in equation (18), and $\mathbf{f}^{\ell}$ in equation (19).

2.10 Stiffness Matrices

The tangent stiffness matrix, defined as $\mathbf{K}_e = \frac{\partial \mathbf{f}_e}{\partial \mathbf{d}_e}$, is the sum of three contributions, *i.e.*,

$$\mathbf{K}_e = \mathbf{K}_e^{matl} + \mathbf{K}_e^{geom} + \mathbf{K}_e^{load} \tag{67}$$

which are described in the following sections.

All element stiffness matrices are constructed using 2-point Gauss integration. This integration rule is exact for geometrically linear analysis (with up to linearly varying section properties), but only approximate for geometrically nonlinear analysis. The reason for using this "reduced" integration rule (instead of, for example, the 3-point rule) for nonlinear analysis, is that it improves solution accuracy without engendering any spurious modes.

2.10.1 Material Stiffness Matrix

The element material stiffness matrix is defined as:

$$\begin{aligned} \mathbf{K}_e^{matl} &= \int_0^L \mathbf{B}^T \widetilde{\mathbf{C}} \mathbf{B} \\ &\approx \frac{L_e}{2} \sum_{g=1}^{2} w_g \left(\mathbf{B}^T(x_g) \widetilde{\mathbf{C}}(x_g) \mathbf{B}(x_g) \right) \end{aligned} \tag{68}$$

where w_g and x_g are defined in Table 3, $\mathbf{B}$ is defined in equation (61), and $\widetilde{\mathbf{C}}$ is defined in equation (26).

2.10.2 Geometric Stiffness Matrix

The element geometric stiffness matrix is defined as:

$$\begin{aligned} \mathbf{K}^{geom_e} &= \int_0^L N_x \mathbf{G}^T \mathbf{G} \\ &\approx \frac{L_e}{2} \sum_{g=1}^{2} w_g \left(N_x(x_g) \mathbf{G}^T(x_g) \mathbf{G}(x_g) \right) \end{aligned} \tag{69}$$

where w_g and x_g are defined in Table 3, N_x is the axial-force stress resultant defined in equation (24), and $\mathbf{G}$ is the displacement gradient interpolation matrix, defined as follows:

$$\overline{\mathbf{u}}_{,x}(x) \;=\; \mathbf{G}(x)\,\mathbf{d}^e \tag{70}$$

where

$$\overline{\mathbf{u}}_{,x} = \begin{Bmatrix} \overline{u}_{,x} \\ \overline{v}_{,x} \\ \overline{w}_{,x} \end{Bmatrix} \qquad \mathbf{G} = \begin{bmatrix} \mathbf{g}^{u,x} \\ \mathbf{g}^{v,x} \\ \mathbf{g}^{w,x} \end{bmatrix} = \begin{bmatrix} \mathbf{g}_1^{u,x} & \mathbf{g}_2^{u,x} \\ \mathbf{g}_1^{v,x} & \mathbf{g}_2^{v,x} \\ \mathbf{g}_1^{2,x} & \mathbf{g}_2^{w,x} \end{bmatrix} \tag{71}$$

in which the nodal blocks of the displacement-derivative interpolation row-matrices, $\mathbf{g}_a$, are defined as follows:

$$\begin{array}{ccc} & & \begin{array}{cccccc} \overline{u}_a & \overline{v}_a & \overline{w}_a & \theta_{xa} & \theta_{ya} & \theta_{za} \end{array} \\ \mathbf{g}_a^{u,x} & = & \left[\begin{array}{cccccc} N^L_{a,x} & 0 & 0 & 0 & 0 & 0 \end{array}\right] \\ \mathbf{g}_a^{v,x} & = & \left[\begin{array}{cccccc} 0 & \overline{N}^H_{a,x} & 0 & 0 & 0 & \widehat{N}^H_{a,x} \end{array}\right] \\ \mathbf{g}_a^{w,x} & = & \left[\begin{array}{cccccc} 0 & 0 & \overline{N}^H_{a,x} & 0 & -\widehat{N}^H_{a,x} & 0 \end{array}\right] \end{array} \tag{72}$$

where the shape functions appearing in equation (72) have been defined in Tables 4 and 5.

The above expression for the geometric stiffness matrix (eq. (69)) neglects terms involving the moment stress resultants, M_y and M_z, but the N_x term is typically dominant. Moreover, when the high-order corotational option is selected, the neglected terms are compensated for by the higher-order stiffness matrix emanating from the corotational projection operator (see Chapter 4 of the Generic Structural-Element Processor Manual (ref. 3) for details).

2.10.3 Load Stiffness Matrix

The load stiffness matrix, defined as $\mathbf{K}_e^{load} = \frac{\partial \mathbf{f}_e^{ext}}{\partial \mathbf{d}_e}$, has not yet been implemented for elements within processor ES6.

2.11 Mass Matrices

All element mass matrices are constructed using 2-point Gauss numerical integration. Note that this represents an extremely *reduced* form of numerical integration, since the Hermitian-cubic polynomial representation of the transverse displacements, $\overline{v}$ and $\overline{w}$, gives rise to a 6th-order polynomial integrand for the mass matrix – and the 2-point Gauss rule is exact only up to 3rd-order integrands. Nevertheless, the use of approximate mass matrices (*e.g.*, employing lower-order displacement interpolation than for the stiffness matrix) is usually adequate, often more accurate for obtaining vibration modes, and of course economical.

2.11.1 Consistent Mass Matrix

The beam element consistent mass matrix emanates from the the kinetic energy, T, which for a continuum may be expressed as:

$$T = \frac{1}{2}\int_V \dot{\mathbf{u}}^T \dot{\mathbf{u}}\, \rho\, dV \tag{73}$$

where $\dot{\mathbf{u}}$ is the the velocity vector, and ρ is the mass density. Substitution of the beam kinematics:

$$\dot{\mathbf{u}}(x,y,z) = \widetilde{\mathbf{A}}(y,z)\,\dot{\tilde{\mathbf{u}}}(x) \tag{74}$$

where:

$$\dot{\tilde{\mathbf{u}}} = \begin{Bmatrix} \dot{\bar{\mathbf{u}}} \\ \dot{\boldsymbol{\theta}} \end{Bmatrix}, \qquad \widetilde{\mathbf{A}} = [\,\mathbf{I}_3 \quad \mathbf{A}\,], \qquad \mathbf{A} = \begin{bmatrix} 0 & z & -y \\ -z & 0 & 0 \\ y & 0 & 0 \end{bmatrix} \tag{75}$$

yields:

$$T = \frac{1}{2}\int_0^L \dot{\tilde{\mathbf{u}}}^T \left(\int_A \widetilde{\mathbf{A}}^T \widetilde{\mathbf{A}}\, \rho\, dA\right) \dot{\tilde{\mathbf{u}}}\, dx \tag{76}$$

Finally, the beam-element mass matrix emerges by substituting the beam-element interpolation approximation for $\dot{\tilde{\mathbf{u}}}(x)$, namely:

$$\dot{\tilde{\mathbf{u}}}(x) = \widetilde{\mathbf{N}}_D(x)\,\dot{\mathbf{d}}^e \tag{77}$$

which gives for the beam-element kinetic energy:

$$T_e = \frac{1}{2}\dot{\mathbf{d}}_e^T\, \mathbf{M}_e\, \dot{\mathbf{d}}_e \tag{78}$$

from which the beam-element mass matrix is identified as:

$$\boxed{\begin{aligned} \mathbf{M}_e &= \int_0^L \widetilde{\mathbf{N}}_D^T \mathcal{I} \widetilde{\mathbf{N}}_D\, dx \\ &\approx \frac{L_e}{2}\sum_{g=1}^{2} w_g \left(\widetilde{\mathbf{N}}_D^T(x_g)\,\mathcal{I}(x_g)\,\widetilde{\mathbf{N}}_D(x_g)\right) \end{aligned} \qquad (79)}$$

where the integrated inertia matrix, $\mathcal{I}(x)$, is defined as follows:

$$\mathcal{I} = \int_A \widetilde{\mathbf{A}}^T(y,z)\,\widetilde{\mathbf{A}}(y,z)\,\rho(y,z)dA \tag{80}$$

For homogeneous materials, $\mathcal{I}$ becomes:

$$\mathcal{I} = \begin{array}{c} \\ \dot{\overline{u}} \\ \dot{\overline{v}} \\ \dot{\overline{w}} \\ \dot{\theta}_x \\ \dot{\theta}_y \\ \dot{\theta}_z \end{array} \begin{array}{c} \begin{array}{cccccc} \dot{\overline{u}} & \dot{\overline{v}} & \dot{\overline{w}} & \dot{\theta}_x & \dot{\theta}_y & \dot{\theta}_z \end{array} \\ \begin{pmatrix} \rho A & 0 & 0 & 0 & \rho A e_z & \rho A e_y \\ & \rho A & 0 & -\rho A e_z & 0 & 0 \\ & & \rho A & \rho A e_y & 0 & 0 \\ & & & \rho J & 0 & 0 \\ & & & & \rho I_z & -\rho I_{yz} \\ sym. & & & & & \rho I_y \end{pmatrix} \end{array} \tag{81}$$

where the cross-section properties, e_y, and e_z, A, I_y, I_z, I_{yz}, and J were defined in equations (28)-(34).

2.11.2 Lumped (Diagonal) Mass Matrix

The E210 beam element diagonal mass matrix is defined as:

$$\mathbf{M}_e = \begin{bmatrix} \mathbf{M}_1^e & \mathbf{0} \\ \mathbf{0} & \mathbf{M}_2^e \end{bmatrix} \tag{82}$$

where each nodal block is defined as follows:

$$
\mathbf{M}_a^e = \int_0^L
\begin{array}{c}
\begin{array}{cccccc}
\dot{\bar{u}}_a & \dot{\bar{v}}_a & \dot{\bar{w}}_a & \dot{\theta}_{xa} & \dot{\theta}_{ya} & \dot{\theta}_{za}
\end{array} \\
\begin{pmatrix}
N_a^L \rho A & & & & & \\
& N_a^L \rho A & & & & \\
& & N_a^L \rho A & & & \\
& & & N_a^L \rho J & & \\
& & & & (\widehat{N}_{a,x}^H)^2 \rho I_{zz} & \\
& & & & & (\widehat{N}_{a,x}^H)^2 \rho I_{yy}
\end{pmatrix}
\end{array}
\tag{83}
$$

where the shape functions N_a^L and $\widehat{N}_{a,x}^H$ are defined in Tables 4 and 5, respectively. Note that this is just the diagonal part of the consistent mass matrix given in equation (79).

2.12 Element Nonlinearity

For nonlinear problems, the discrete system of equations given in equation (42) generalizes to (ignoring structural damping and higher-order inertial effects):

$$\mathbf{M}\ddot{\mathbf{d}} + \mathbf{f}^{int}(\mathbf{d}) = \mathbf{f}^{ext}(\mathbf{d},\lambda) \tag{84}$$

where $\mathbf{f}^{int}$ and $\mathbf{f}^{ext}$ are now *nonlinear* vector operators. This equation system is then *linearized*, yielding the following linear equation system to be solved at each iteration of a nonlinear analysis:

$$\mathbf{M}\,\delta\ddot{\mathbf{d}} + \mathbf{K}\,\delta\mathbf{d} = \mathbf{f}^{ext}(\mathbf{d},\lambda) - \mathbf{f}^{int}(\mathbf{d}) \tag{85}$$

where $\mathbf{d}$ is the displacement vector connecting the current (reference) configuration to the initial configuration, $\delta\mathbf{d}$ is the iterative change in the displacement vector (to be computed), and $\mathbf{K}$ is the tangent stiffness matrix at either the current configuration (for True-Newton iteration) or some previous configuration (for Modified-Newton iteration).

The nonlinear ES6 element contributions to $\mathbf{M}$, $\mathbf{K}$, $\mathbf{f}^{ext}$ and $\mathbf{f}^{int}$ have the same form as the linear contributions, with the following exceptions:

1) The stress resultant array, $\tilde{\sigma}$, which appears explicitly in both $\mathbf{f}^{int}$ and in $\mathbf{K}^{geom}$ is computed using the *Green-Lagrange* strain tensor $\mathbf{E}$ defined as follows:

$$\mathbf{E} = \frac{1}{2}\left[\frac{\partial \mathbf{u}}{\partial \mathbf{X}} + \left(\frac{\partial \mathbf{u}}{\partial \mathbf{X}}\right)^T + \left(\frac{\partial \mathbf{u}}{\partial \mathbf{X}}\right)^T \frac{\partial \mathbf{u}}{\partial \mathbf{X}}\right] \tag{86}$$

where $\mathbf{X}$ are the coordinates in the *undeformed* configuration. To simplify the formulation, the nonlinear terms in $\mathbf{u}$ are added only to the beam *axial* strain, $\bar{\epsilon}_x$. Thus, in geometrically nonlinear analysis, the linear axial strain, $\bar{\epsilon}_X = \partial\bar{u}/\partial X$, is replaced with the following definition:

$$\bar{\epsilon}_X \longleftarrow \bar{\epsilon}_x + \bar{\epsilon}_x^{NL} \tag{87}$$

where

$$\bar{\epsilon}_X^{NL} = \frac{1}{2}(\bar{u}_{,X}^2 + \bar{v}_{,X}^2 + \bar{w}_{,X}^2) \tag{88}$$

where X denotes the *undeformed* axial coordinate in the initial element Cartesian frame, and $\bar{u},\bar{v},\bar{w}$ are the total displacements expressed in this same initial basis. The displacement derivatives are computed using:

$$\begin{aligned} \bar{u}_{,X} &= \sum_{a=1}^{2} \mathbf{g}_a^{u,x}\,\mathbf{d}_a \\ \bar{v}_{,X} &= \sum_{a=1}^{2} \mathbf{g}_a^{v,x}\,\mathbf{d}_a \\ \bar{w}_{,X} &= \sum_{a=1}^{2} \mathbf{g}_a^{w,x}\,\mathbf{d}_a \end{aligned} \tag{89}$$

where the gradient interpolation matrices, $\mathbf{g}_a$, were defined in equation (72). Once $\bar{\epsilon}_X^{NL}$ has been added to the linear strains, as in equation (87), the stress resultants can then be computed from the total strains in the same way as during geometrically linear analysis; *e.g.*, for linear-elastic materials:

$$\tilde{\sigma} = \tilde{\mathbf{C}}\tilde{\epsilon} \tag{90}$$

2) When the strain-displacement relations become nonlinear, the $\mathbf{B}$ matrix appearing in the element internal force and material stiffness arrays, $\mathbf{f}_e^{int}$ and $\mathbf{K}_e^{matl}$, also has to be modified. For nonlinear analysis, the $\mathbf{B}$ matrix represents an *incremental* relation between interior strains and nodal displacements, *i.e.*,

$$\delta\tilde{\epsilon}(\xi,\eta) = \mathbf{B}(\xi,\eta;\bar{\mathbf{u}})\,\delta\mathbf{d}^e \tag{91}$$

where

$$\delta\mathbf{d}_a = \begin{Bmatrix} \delta\bar{u}_a \\ \delta\bar{v}_a \\ \delta\bar{w}_a \\ \delta\theta_{Xa} \\ \delta\theta_{Ya} \\ \delta\theta_{Za} \end{Bmatrix} \tag{92}$$

are the *nodal displacement increments* at node a, and $\bar{\mathbf{u}}$ is the total displacement vector in the interior of the element. As in the case of total strain calculation, the nonlinear contributions to the incremental strains are added only to the axial component. Thus we replace the linear axial strain increment as follows:

$$\delta\bar{\epsilon}_X \longleftarrow \delta\bar{\epsilon}_X + \delta\bar{\epsilon}_X^{NL} \tag{93}$$

where

$$\delta\bar{\epsilon}_X^{NL} = \bar{u}_{,X}\delta\bar{u}_{,X} + \bar{v}_{,X}\delta\bar{v}_{,X} + \bar{w}_{,X}\delta\bar{w}_{,X} \tag{94}$$

Substituting the displacement approximations into the above equation leads to the corresponding nonlinear contribution to the $\mathbf{B}$ matrix; that is, we replace:

$$\mathbf{B}^{\bar{\epsilon}_X} \longleftarrow \mathbf{B}^{\bar{\epsilon}_X} + \mathbf{B}^{\bar{\epsilon}_X^{NL}} \tag{95}$$

where

$$\boxed{\begin{array}{c} \mathbf{B}_a^{\bar{\epsilon}_X^{NL}}(\xi,\eta) = \\[6pt] \begin{array}{cc} & \begin{array}{cccccc} \bar{u}_a & \bar{v}_a & \bar{w}_a & \theta_{Xa} & \theta_{Ya} & \theta_{Za} \end{array} \\ \delta\bar{\epsilon}_X & \begin{pmatrix} \bar{u}_{,X}N_{a,X}^L & \bar{v}_{,X}\overline{N}_{a,X}^H & \bar{w}_{,X}\overline{N}_{a,X}^H & 0 & -\bar{w}_{,X}\widehat{N}_{a,X}^H & \bar{v}_{,X}\widehat{N}_{a,X}^H \end{pmatrix} \end{array} \end{array}} \tag{96}$$

in which N_a^L and $(\overline{N}_a^H, \widehat{N}_a^H)$ are the Lagrange and Hermite interpolation functions defined in Tables 4 and 5. Note that the row of the nonlinear **B** matrix corresponding to $\overline{\epsilon}_X$ now couples all of the element nodal freedoms except for the torsional rotations, θ_{xa} , whereas the linear counterpart involves only the axial displacements, $\overline{u}_a$.

3) All of the element integrals, *e.g.*, for stiffness matrices and force vectors, are carried out over the *initial* (undeformed) element domain. The effect of large rotations is accounted for using $\overline{\epsilon}_X^{NL}$ and $\mathbf{B}^{\overline{\epsilon}_X^{NL}}$, defined above.

4) For very large rotations, the *corotational* facility built-in to the generic element processor shell (ES) may be used. In this case the bulk rigid body motion of each element is first "subtracted" from the overall motion before computing $\mathbf{K}_e$, $\mathbf{f}_e^{int}$, and $\widetilde{\sigma}(\widetilde{\epsilon})$. The main effect of this adjustment is to increase the accuracy of the nonlinear strain-displacement relations (eq. (97)), since the nonlinear terms in the Green-Lagrange strain tensor, *i.e.*, $\overline{\epsilon}_X^{NL}$, become small after the element's rigid body motion has been subtracted, and the accuracy continues to increase as the beam-element mesh is refined. In fact, with the corotational option on, it is even possible to solve nonlinear problems without using any other element nonlinearity (albeit with a lower order of accuracy). See reference 2 for details.

4) The element external force vector, $\mathbf{f}_e^{ext}$, is a nonlinear function of the displacement vector, $\mathbf{d}_e$, only if *live* (*e.g.*, hydrostatic) loads are present. For displacement-independent (*i.e.*, *dead*) loads, the external force vector is usually expressible as:

$$\mathbf{f}^{ext} = \lambda \widehat{\mathbf{f}}^{ext} \tag{97}$$

where $\widehat{\mathbf{f}}^{ext}$ is a fixed base load vector, and λ is the current load factor. In this case, equation (85) is evaluated only once (initially), and scaled by λ as the analysis progresses.

2.13 Modifications to Include Transverse-Shear Deformation

An expedient option exists to include transverse-shear deformations in the basic ES6/E210 beam-element formulation – for *linear* analysis only. This option captures the effect of linear Timoshenko beam theory, by augmenting the strain-displacement matrix, **B**, and the constitutive matrix, $\widetilde{\mathbf{C}}$, by two new rows.

Hence, each 4 × 6 nodal block of the **B** matrix is replaced by a 6 × 6 nodal block, as follows:

$$\boxed{\mathbf{B}_a \longleftarrow \mathbf{B}_a^*} \tag{98}$$

where

$$\boxed{\mathbf{B}_a^* = \begin{array}{c} \\ \bar{\epsilon}_x \\ \kappa_y \\ \kappa_z \\ \alpha \\ \kappa_y^* \\ \kappa_z^* \end{array} \begin{array}{c} \begin{array}{cccccc} \overline{u}_a & \overline{v}_a & \overline{w}_a & \theta_{xa} & \theta_{ya} & \theta_{za} \end{array} \\ \begin{pmatrix} N_{a,x}^L & 0 & 0 & 0 & 0 & 0 \\ 0 & 0 & -\overline{N}_{a,xx}^H & 0 & \widehat{N}_{a,xx}^H & 0 \\ 0 & -\overline{N}_{a,xx}^H & 0 & 0 & 0 & -\widehat{N}_{a,xx}^H \\ 0 & 0 & 0 & N_{a,x}^L & 0 & 0 \\ 0 & 0 & 0 & 0 & -\frac{(-1)^a}{L_e} & 0 \\ 0 & 0 & 0 & 0 & 0 & \frac{(-1)^a}{L_e} \end{pmatrix} \end{array}} \tag{99}$$

The new rows for κ_y^* and κ_z^* denote constant curvature corrections to the basic curvatures, κ_y and κ_z – to account for transverse-shear deformation. Thus, equation (99) yields:

$$\begin{aligned} \kappa_y^* &= \frac{\theta_{y2} - \theta_{y1}}{L_e} \\ \kappa_z^* &= -\frac{\theta_{z2} - \theta_{z1}}{L_e} \end{aligned} \tag{100}$$

where θ_{ya} and θ_{za} are the nodal rotations.

Correspondingly, the 4×4 resultant constitutive matrix, $\widetilde{\mathbf{C}}$, is replaced by a 6×6 matrix, as follows:

$$\boxed{\widetilde{\mathbf{C}} \longleftarrow \widetilde{\mathbf{C}}^*} \tag{101}$$

where:

$$\boxed{\widetilde{\mathbf{C}}^* = \begin{array}{c} \\ N_x \\ M_y \\ M_z \\ T \\ M_y^* \\ M_z^* \end{array} \begin{array}{c} \begin{array}{cccccc} \bar{\epsilon}_x & \kappa_y & \kappa_z & \alpha & \kappa_y^* & \kappa_z^* \end{array} \\ \begin{pmatrix} EA & EAe_z & EAe_y & 0 & 0 & 0 \\ EAe_z & \frac{EI_{zz}}{1+\phi_z} & EI_{yz} & 0 & 0 & 0 \\ EAe_y & EI_{yz} & \frac{EI_{yy}}{1+\phi_y} & 0 & 0 & 0 \\ 0 & 0 & 0 & GJ & 0 & 0 \\ 0 & 0 & 0 & 0 & \frac{\phi_z EI_{zz}}{1+\phi_z} & 0 \\ 0 & 0 & 0 & 0 & 0 & \frac{\phi_y EI_{yy}}{1+\phi_y} \end{pmatrix} \end{array}} \tag{102}$$

in which:

$$\begin{aligned} \phi_y &= \frac{12EI_{yy}}{G\alpha_y A L_e^2} \\ \phi_z &= \frac{12EI_{zz}}{G\alpha_z A L_e^2} \end{aligned} \tag{103}$$

where α_y and α_z are transverse-shear correction factors for bending in the $x-y$ and $x-z$ planes, respectively.

The transverse-shear option is activated by setting α_y or α_z to a number between 0 and 1, *e.g.*, 5/6 to match Reissner's theory. If these parameters are both set to 0, the transverse-shear option is bypassed.*

* Note: Currently, the transverse-shear option has not been activated in the CSM Testbed. A modification to the element cover routines for processor ES6 is required in order to convey these parameters to the E210 element kernel routines.

3. REFERENCES

1. Stewart, Caroline B., Compiler: *The Computational Structural Mechanics Testbed User's Manual.* NASA TM-100644, October, 1989.

2. Almroth, B.O., Brogan, F.A. and Stanley, G.M.: *Structural Analysis of General Shells, Vol. II: User Instructions for the STAGS(C-1) Computer Code*, NASA CR-165671, 1981.

3. Stanley, Gary and Nour-Omid, Shahram: *The Computational Structural Mechanics Testbed Generic Structural-Element Processor Manual.* NASA CR-181728, 1990.

NASA
National Aeronautics and Space Administration

Report Documentation Page

1. Report No.	2. Government Accession No.	3. Recipient's Catalog No.
NASA CR-4359		

4. Title and Subtitle The Computational Structural Mechanics Testbed Structural Element Processor ES6: STAGS Beam Element	5. Report Date May 1991
	6. Performing Organization Code
7. Author(s) Shahram Nour-Omid, Frank Brogan and Gary M. Stanley	8. Performing Organization Report No. LMSC-D878511
9. Performing Organization Name and Address Lockheed Missiles & Space Company, Inc. Research and Development Division 3251 Hanover Street Palo Alto, California 94304	10. Work Unit No. 505-63-53-01
	11. Contract or Grant No. NAS1-18444
12. Sponsoring Agency Name and Address National Aeronautics and Space Administration Langley Research Center Hampton, VA 23665-5225	13. Type of Report and Period Covered Contractor Report
	14. Sponsoring Agency Code

15. Supplementary Notes
Langley Technical Monitor: Jerrold M. Housner

16. Abstract
The purpose of this manual is to document the theory behind the CSM Testbed structural finite element processor ES6 for the STAGS beam element. This report is intended both for CSM Testbed users, who would like theoretical background on element types before selecting them for an analysis, as well as for element researchers who are attempting to improve existing elements or to develop entirely new formulations.

Processor ES6 contains the displacement-based 2-node beam element used within the STAGS code (ref. 2). This element is intended for modeling slender beams, which appear either in frame structures or as stiffening elements for shell structures. In STAGS, the element is referred to as the 210 element; in CSM Testbed processor ES6, it is called element E210. The E210 element in ES6 is a two-node *straight* beam element with 3 translational and 3 rotational freedoms per node. It thus represents a *faceted* approximation when used to model curved structures. The element features a cubic transverse (bending) displacement field, and linear axial and torsional displacement fields. Hence, it is considered compatible as a stiffener element with the STAGS-410 shell element, which is implemented as element E410 in CSM Testbed processor ES5. Note that the E210 beam element does not model warping deformations due to torsion, but does have a limited transverse-shear deformation capability (described in Section 2.13).

Arbitrarily large rotations (but only small strains) may be modeled with these elements by employing the standard corotational utility available for all ES processors.

17. Key Words (Suggested by Authors(s))	18. Distribution Statement
Structural analysis software Finite Element Implementation Corotational Formulation CSM Testbed System	Unclassified—Unlimited Subject Category 39

19. Security Classif.(of this report)	20. Security Classif.(of this page)	21. No. of Pages	22. Price
Unclassified	Unclassified	38	A03

NASA FORM 1626 OCT 86

For sale by the National Technical Information Service, Springfield, Virginia 22161-2171

NASA-Langley, 1991